CHEMISTRY OF MATERIALS

Article

pubs.acs.org/cm

Brominated Chemistry for Chemical Vapor Deposition of Electronic Grade SiC

Milan Yazdanfar, Örjan Danielsson, Emil Kalered, Pitsiri Sukkaew, Olle Kordina, Daniel Nilsson, Ivan G. Ivanov, Lars Ojamäe, Erik Janzén, and Henrik Pedersen*

Department of Physics, Chemistry and Biology, Linköping University, SE-581 83 Linköping, Sweden

Supporting Information

ABSTRACT: Chlorinated chemical vapor deposition (CVD) chemistry for growth of homoepitaxial layers of silicon carbide (SiC) has paved the way for very thick epitaxial layers in short deposition time as well as novel crystal growth processes for SiC. Here, we explore the possibility to use a brominated chemistry for SiC CVD by using HBr as additive to the standard SiC CVD precursors. We find that brominated chemistry leads to the same high material quality and control of material properties during deposition as chlorinated chemistry and that the growth rate is on average 10% higher for a brominated chemistry compared to chlorinated chemistry. Brominated and chlorinated SiC CVD also show very similar gas-phase chemistries in thermochemical modeling. This study thus argues that brominated chemistry is a strong alternative for SiC CVD because the deposition rate can be increased with preserved material quality. The thermochemical modeling also suggest that the currently used chemical mechanism for halogenated SiC CVD might need to be revised.

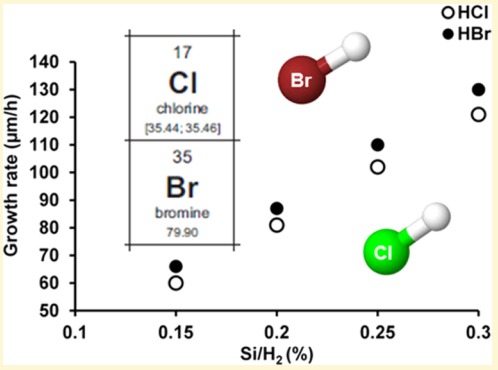

INTRODUCTION

Silicon carbide (SiC) is an excellent semiconductor material with unique properties that provide it with significant advantages over existing Si and III−V technologies. The advantages lies in the material properties in the form of a wide band gap of around 3 eV, high breakdown electric field strength, high thermal conductivity and high saturation electron drift velocity.[1] The breakdown electric field is about ten times higher than for Si, allowing SiC power diodes to have ten times thinner blocking layers,[2] and the many orders of magnitude lower intrinsic carrier concentration for SiC than Si, allows for significantly higher operating temperatures for SiC devices as compared to Si devices. Thus, SiC has the potential to replace current materials in most high-frequency and high-power devices,[2] and can dramatically reduce power losses in most distribution and generation systems for electrical energy as well as in electrical motors.

The still relatively high production cost of a SiC device is due to the fabrication technique. Fabrication of SiC-based power devices requires growth of a homoepitaxial layer, with well-controlled doping level and thickness, which will serve as the active region of the device. Chemical vapor deposition (CVD) is the standard method for homoepitaxial SiC growth, typically using silane (SiH_4) and propane or ethylene diluted in hydrogen at 1500−1600 °C with a growth rate of 5−10 μm/h.[3] As an example, a SiC blocking device for 10 kV requires 100 μm thick epitaxial layer,[4] therefore an increased growth rate is of outmost importance for reducing the production costs of SiC devices. Increasing the growth rate can, in principle, be done by increasing the precursor concentration in the CVD gas mixture. However, this will lead to unwanted formation of silicon clusters in the gas phase that can lead to detrimental surface defects in the SiC layer.[5] This problem can be circumvented by physical methods such as adding more energy to the system to dissolve the silicon clusters[6] or lower the probability for silicon clusters to form by lower the silicon partial pressure by lowering the total pressure.[7] Addition of chlorine to the precursor gases is a chemical remedy to the formation of silicon clusters. This method has been studied and developed for SiC homoepitaxial CVD for the last approximately 10 years and enabled growth rates exceeding 100 μm/h, paving the way for very thick homoepitaxial SiC layers in short deposition time and novel processes for growth of bulk SiC crystals.[8] The rationale is that the strong Si−Cl bond (417 kJ/mol or 4.32 eV) prevents Si−Si bonds (310 kJ/mol or 3.21 eV)[9] from forming.

Given the often very similar chemistries of molecules with different halogen atoms, it is of interest to study how other halogenated growth chemistries beside chlorinated behaves. Fluorinated and brominated chemistry could be expected to work, given the Si−F (576 kJ/mol or 5.97 eV) and Si−Br (358 kJ/mol or 3.71 eV) bond strengths, whereas the Si−I bond (234 kJ/mol or 2.52 eV) that has lower bond strength than the Si−Si bond would be expected to be less efficient. A recent comparison between chlorinated and fluorinated chemistry for

Received: October 1, 2014
Published: January 22, 2015

DOI: 10.1021/acs.chemmater.5b00074
Chem. Mater. 2015, 27, 793−801

homoepitaxial growth of SiC has been reported, indicating higher suppression of gas-phase nucleation with fluorinated chemistry.[10] For brominated chemistry, two papers from 1995 comparing methyl trichlorosilane, CH_3SiCl_3 (MTCS), and methyl tribromosilane, CH_3SiBr_3 (MTBS), can be found; however, these reported on heteroepitaxial growth of cubic SiC on silicon substrates.[11,12] Heteroepitaxial growth presents a different set of challenges compared to homoepitaxial growth and use of silicon substrates also sets a strict upper temperature in the melting point of Si, 1414 °C. Nevertheless, ref 11 reports a higher growth rate but lower material quality for brominated chemistry compared to chlorinated chemistry. The data presented indicate lower activation energy for the CVD process with brominated chemistry, whereas the lower material quality of SiC from MTBS is ascribed to lower precursor purity.[11] The higher growth rate and possibly lower activation energy for heteroepitaxial growth raises the question if brominated chemistry can outperform chlorinated chemistry in homoepitaxial growth of SiC.

In this study, we seek to compare chlorinated and brominated chemistry for homoepitaxial growth of hexagonal SiC by making a direct comparison using either HCl or HBr as additive to the standard SiC CVD gas mixture. We compare the two chemistries by homoepitaxial growth experiments, thermochemical calculations of the gas phase chemistry, and quantum chemical modeling of the surface chemistry.

METHODS

Experimental Details. Homoepitaxial growth experiments were done in a horizontal hot wall CVD reactor without rotation of the substrate, conceptually described in detail by Henry et al.,[13] using SiH_4 and C_2H_4 as Si- respectively C-precursors diluted in a hydrogen carrier gas flow of 50 l/min with HCl or HBr as growth additives and no intentional dopants added to the gas mixture. The SiH_4 flow for a Si/H_2 ratio of 0.25% was 125 sccm and the HCl or HBr flow for a (Cl or Br)/Si of 4 was 500 sccm. Single crystalline SiC substrates are only available in the hexagonal polytypes 4H and 6H, therefore homoepitaxial growth of SiC for device applications must be done on these polytypes. Here, 4H-SiC single crystalline substrates using approximately 15 × 15 mm^2 pieces cut from one chemo mechanically polished 150 mm, 4H-SiC wafer with 4° off-cut toward the [11−20] direction was used. The growth experiments were performed on the (0001) surface, also known as the Si-face, of the substrate. The precursor concentration in the gas mixture, Si/H_2, was varied by changing the precursor flows keeping the C/Si and (Cl or Br)/Si ratios constant. The (Cl or Br)/Si ratio was varied by changing only the HCl or HBr flow and the C/Si ratio was varied by changing only the C_2H_4 flow. For all experiments, the growth temperature, growth pressure and growth time were kept constant at 1575 °C, 100 mbar and 15 min, respectively. Experiments to estimate the etching rate of HCl and HBr addition were done by placing grown epitaxial layers with known thickness in the CVD reactor and subjecting them to a flow of hydrogen, 50 L/min, and HCl or HBr, 500 mL/min, for 60 min at growth conditions, 1575 °C and 100 mbar.

The safety aspects of using HBr as additive to CVD of SiC are very much the same as when using HCl; the HBr gas bottle should be installed in a ventilated gas cabinet equipped with HBr sensitive gas detector, gas mask able to filtrate HBr should be used when loading and unloading the samples, HBr sensitive gas detector should be installed in the lab close to the loading port of the CVD reactor and a scrubber capable of removing residual HBr and Br_2 should be installed to clean the exhaust gases. The close similarities between Cl and Br chemistry mean that equipment suitable for chlorinated SiC CVD is often also suitable for brominated SiC CVD.

The thickness of the epitaxial layers was measured using Fourier transform infrared (FTIR) reflectance and the surface morphology of the epitaxial layers was studied by an optical microscope with Nomarski differential interference contrast, and by atomic force microscopy (AFM) in tapping mode on 20 × 20 μm^2 areas at the center of the substrate and at two different spots about 2 mm from the sample edge. The net carrier concentration of the grown epitaxial layers was determined from capacitance−voltage (CV) measurement using a mercury probe. The material quality of the grown epitaxial layers was studied by (i) low temperature photoluminescence (LTPL) at 2 K with a frequency doubled Argon ion laser at 244 nm, and (ii) by high resolution X-ray diffraction (HRXRD) using a triple axis diffractometer equipped with a 4-bounce Ge(220) symmetrical optics using a 5 × 5 mm^2 X-ray slit opening (corresponding to a footprint of ∼5 × 16 mm^2 for the 4H-SiC(0004) peak) and 3-bounce Ge(220) symmetrical analyzer. Possible bromine and chlorine incorporation in the grown epitaxial layers was investigated by secondary ion mass spectrometry (SIMS) by Evans Analytical Group (EAG) East Windsor, New Jersey, USA using a Cs^+ primary ion beam, detecting negative secondary ions.

Thermochemical Modeling. Calculations of thermodynamic equilibrium, based on minimization of Gibbs free energy, for the Si−C−Cl−H and Si−C−Br−H systems were made for the temperature range 100−1700 °C and a pressure of 100 mbar. The composition of the gas mixture was Si/H_2 = 0.25%, C/Si = 1.0 and (Cl or Br)/Si = 4.0. Because the calculations are based on equilibrium thermodynamics, it is implied that the final result is independent of the initial form of the elements. Included in the study were 23 silicon hydrides (Si_xH_y) with up to 5 silicon atoms, 37 hydrocarbons with up to 5 carbon atoms, 36 Si−C molecules ($Si_xC_yH_z$), Si_x (x = 1−6), C_x (x = 1−6), and 16 small Si−C clusters: Si_xC_y (from $x + y$ = 2 up to $x + y$ = 6). The thermochemical data for these molecules needed for the calculations were taken from literature.[14] In addition all 10 + 10 combinations of SiH_yX_z and CH_yX_z molecules (X = Cl or Br, y = 0−3, z = 1−4) were included. The thermochemical data for these molecules were determined from quantum chemical calculations and are given in the Supporting Information and will also be presented in a separate publication. For the chlorinated chemistry, an additional 39 molecules containing chlorine (and hydrogen) plus two Si + C atoms (i.e., two Si, two C or one Si + one C) were included.[15] A list of all species included in the study can be found in the Supporting Information. Because of a lack of thermochemical data, the corresponding 39 bromine containing molecules could not be included for calculations of the Si−C−Br−H system. It should be pointed out that in the Si−C−Cl−H system, the mole fractions of these 39 species were well below 1 × 10^{-8}, except for Si_2Cl_6, Si_2Cl_5H, Cl_3SiCH_3, HCl_2SiCH_3, and $ClSiCH_3$ at temperatures below 1200 °C, where mole fractions up to 1 × 10^{-6} could be noted. It could therefore be assumed that the corresponding bromine containing molecules would also have low concentrations in equilibrium in the temperature region of interest here, 1400−1700 °C.

In SiC CVD, which is done at a relatively high temperature, it is presumed that gas-phase reactions are fast, and that mass transport to the surface is the limiting step. Estimations of the different time scales show that the mean time between molecular impacts on a surface site (i.e., mass transport) is in general 1 × 10^3 to 1 × 10^8 times longer than the chemical-reaction (gas-phase and surface) times.[16] Thus, the assumption that the gas may reach chemical equilibrium can be used as a good approximation, even though there might be some reaction steps that are slower. Only gas-phase species were considered in the calculations (no solid or liquid phases were included). This assumption is valid in cases where mass transport to the surface or surface reactions are rate-limiting, allowing the gas-phase to reach equilibrium (i.e., gas-phase reactions are fast enough). However, if gas-phase nucleation actually occurs, this does not show in such calculations. Therefore, the inclusion of the "larger" Si_x, C_x, and Si_xC_y molecules could here be considered to represent small particles formed by nucleation in the gas and an indication that gas-phase nucleation might occur.

The number of molecules that hits a unit area of the surface per unit time is used as a simplified measure of the growth rate (assuming all molecules that hit the surface also will be incorporated in the epitaxial layer). To determine the molecular hit-rate the Maxwell−Boltzmann

DOI: 10.1021/acs.chemmater.5b00074
Chem. Mater. 2015, 27, 793−801

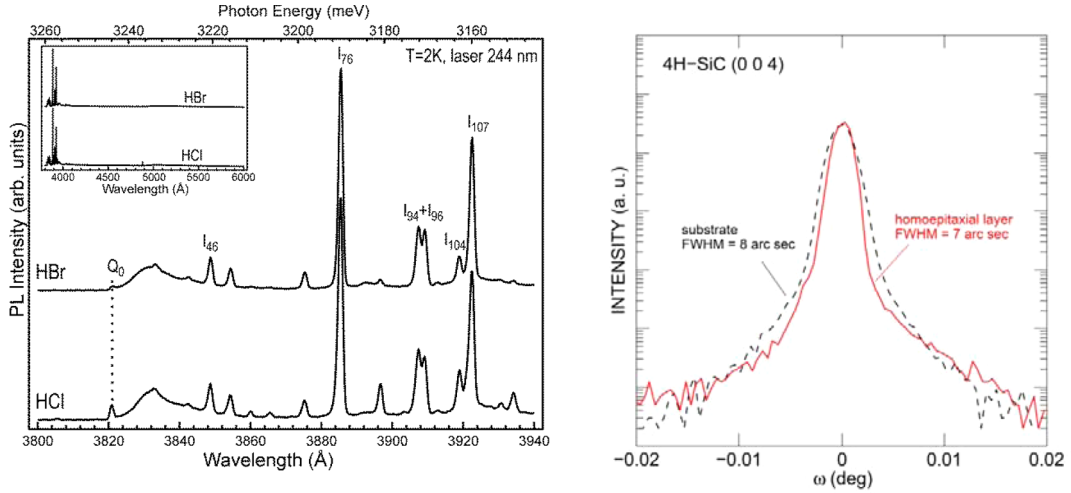

Figure 1. Material quality of epitaxial SiC layers grown with brominated chemistry. (a) Typical LTPL spectra of layers grown with C/Si = 1 and Si/H_2 = 0.30% using chlorinated (Cl/Si = 4, growth rate 120 μm/h) and brominated chemistries (Br/Si = 4, growth rate 130 μm/h), as indicated for each spectrum. The spectra are completely dominated by the free-exciton phonon replicas, some of which are denoted in a common notation by I and a subscript indicating the energy of the phonon (in meV) involved in the recombination. The inset displays the same spectra in the whole spectral region measured; the weak peak at ∼4880 Å is the second order of the exciting laser line (244 nm) scattered from the sample. The residual n-type doping estimated from the LTPL measurement is 9×10^{13} cm^{-3} for the chlorinated chemistry and 1×10^{14} cm^{-3} for the brominated chemistry. (b) HRXRD ω-scans of the 4H-SiC (0004) XRD peak of a bare substrate and a 23 μm thick epitaxial layer grown at 90 μm/h. The fwhm is 7 arcsec for the epitaxial layer. An X-ray slit opening of 5×5 mm^2, corresponding to a footprint of $\sim 5 \times 16$ mm^2 for the 4H-SiC(0004) peak, was used.

velocity distribution can be used, which leads to the hit-rate expressed in [mol/m^2 s] as

$$\Phi = \frac{p_i}{\sqrt{2\pi M_i RT}} \quad (1)$$

where p_i is the partial pressure of species i, and M_i is the molecular mass of the same species. The partial pressures are given by the thermodynamic equilibrium calculations, and comparison between the growth rates of the chlorinated and brominated chemistries are easily made.

Quantum Chemical Modeling. The surface chemistry of homoepitaxial SiC growth with chlorinated and brominated chemistries was studied by quantum chemical modeling by the same approach as reported by Kalered et al.,[17] using the hydrogen-terminated 4H−SiC (000−1) surface of a small cluster of atoms, cut from the bulk crystal structure. The quantum-chemical calculations were performed using the B3LYP hybrid ab initio density functional theory method[18] with the 6-31G(d,p) basis set[19] in the Gaussian 09 program.[20] A small test of the performance of the functional and basis set for Br was carried out, in which the reaction energy and enthalpy for formation of $SiBr_4$ from SiH_4 and Br_2 was computed. The computed reaction enthalpy using the present functional and basis set was −523 kJ/mol, which is in fair agreement with the value −511 kJ/mol obtained from standard experimental thermodynamic data.[21] The computed reaction energy (i.e., internal energy at 0 K where vibrational zero-point energy is neglected) of −514 kJ/mol also agrees well with the value −509 kJ/mol obtained from calculations using the coupled-cluster method (CCSD(T)) and a nearly complete basis set (aug-cc-pVQZ).[20] Transition-state energies and structures were obtained using the synchronous transit-guided quasi-Newton (STQN) method[22] in the Gaussian 09 program, which uses a quadratic synchronous transit (QST) approach[23] followed by a quasi-Newton algorithm. The adsorption and activation energies for surface reactions for SiH_2 (standard CVD chemistry) and $SiCl_2$ (chlorinated CVD-chemistry) on the (000−1) 4H-SiC surface have previously been studied,[17] and have here been calculated also for $SiBr_2$ allowing us to extend the comparison between SiH_2 and $SiCl_2$ to include also $SiBr_2$.

RESULTS AND DISCUSSION

Homoepitaxial Growth with Chlorinated and Brominated Chemistry. LTPL has the ability to highlight possible crystalline defects affecting the electronic properties in the homoepitaxially grown SiC. Typical PL spectra in the near-band gap region from the chlorinated and brominated chemistries are displayed in Figure 1a. The insert presents an overview of the spectra in the whole spectral region measured and shows that the spectra are entirely dominated by the near-band gap emission. The latter usually comprises the phonon replicas of the nitrogen-bound and free excitons with relative contribution depending on (and often used to estimate) the doping level.[24] However, for both spectra displayed in Figure 1a the only discernible contribution from the nitrogen-bound excitons is the weak appearance of the well-known Q_0 line (this line usually dominates the emission from nitrogen-bound excitons and is associated with direct, i.e., without phonon assistance recombination of excitons bound to nitrogen at a cubic lattice site). Thus, the near-band gap emission is strongly dominated by the phonon replicas of the free exciton, indicating very low unintentional doping (around 1×10^{14} cm^{-3}). We notice that the appearance of the broad bands serving as background in the spectrum (e.g., the band peaking around 3832 Å) is entirely due to emission from the substrate, typically observed with thin (∼15−30 μm) epitaxial layers. No differences in material quality, except for the incorporation of dopants, can be seen by LTPL when varying the growth parameters as described below. HRXRD ω-scan rocking curve measurements were performed on epitaxial layers grown by brominated chemistry, the rocking curve from the (0004) plane is shown in Figure 1b. The full width at half-maximum (fwhm) of the ω-scan rocking curve peak is 7 arcsec indicating high crystalline quality of the epitaxial layer. The width of the $2\theta/\omega$ scan peak is 20 arcsec suggesting low strain in the material. The HRXRD measurements shows that the crystalline quality is high and well in line with previously reported 4H-SiC epitaxial

DOI: 10.1021/acs.chemmater.5b00074
Chem. Mater. 2015, 27, 793−801

layers grown by chlorinated chemistry.[25] LTPL and HRXRD thus suggest that the material quality of epitaxial layers grown by brominated chemistry is as high as of epitaxial layers grown by chlorinated chemistry.

The growth rate of homoepitaxial 4H-SiC layers at (Cl or Br)/Si=4 and C/Si=1, increases linearly when the precursor concentration in the carrier gas, expressed as the Si/H_2 ratio, was increased from 0.15% to 0.30% (Figure 2). Growth rates

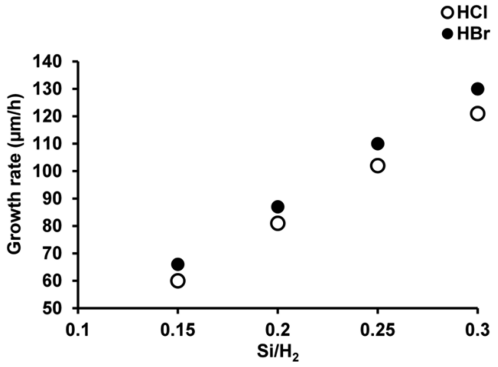

Figure 2. Dependence of growth rate on the Si/H_2 ratio with C/Si=1 and (Cl or Br)/Si = 4 for chlorinated and brominated chemistry for 4H-SiC epitaxial growth.

between 60 and 130 μm/h for both chlorinated and brominated growth chemistry show that brominated chemistry allows the same range of growth rates for homoepitaxial growth of 4H-SiC as chlorinated chemistry. It can also be noted that the growth rate is on average 10% higher for a Br-based chemistry compared to a Cl-based chemistry at the same growth conditions. This could be speculated to be an effect of a lower activation energy as previously suggested[11] or an effect of easier removal of halogen atoms from Si−(Cl or Br) species adsorbed on the SiC surface given the somewhat weaker Si−Br bond.

A key parameter in CVD of electronic grade SiC is the C/Si ratio in the gas mixture because it controls the amount of incorporated dopants.[26] The incorporation of unintentional dopants, expressed as the net carrier concentration ($N_d - N_a$) from capacitance−voltage measurements, in the epitaxial layers grown at C/Si ratio between 0.6 and 1 follows the well-known site competition theory[27] (Figure 3). All epitaxial layers grown in this study are n-type doped in the 1×10^{14} cm^{-3} range, well

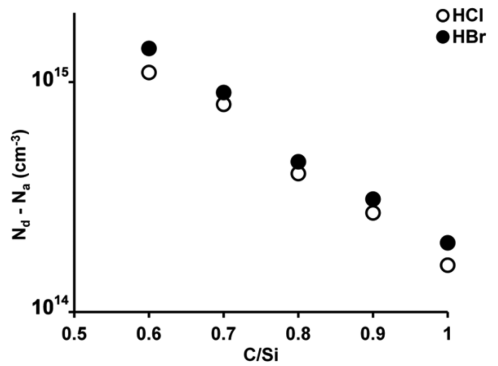

Figure 3. Dependence of net carrier concentration ($N_d - N_a$) caused by background doping, on the C/Si ratio with Si/H_2 = 0.25% and (Cl or Br)/Si = 4 for chlorinated and brominated chemistry for 4H-SiC epitaxial growth.

in line with the doping level that can be estimated from LTPL measurements.[24] The dopant is most likely residual nitrogen emanating from exposing the deposition chamber to air when unloading and loading samples. A slightly higher background doping is measured for epitaxial layers grown by brominated chemistry. This could be attributed to a more efficient Si supply to the growth surface; since nitrogen replaces carbon in the SiC lattice,[28] a more efficient supply of silicon by brominated growth chemistry makes more carbon sites available for nitrogen incorporation.

The variation of the C/Si ratio between 0.6 and 1, keeping a Si/H_2 ratio of 0.25% and a (Cl or Br)/Si ratio of 4, also shows the classical dependence of growth rate on C/Si where the growth rate decreases with more silicon rich conditions and evens out with more carbon-rich conditions,[29] for both Br- and Cl-based chemistry, Figure 4.

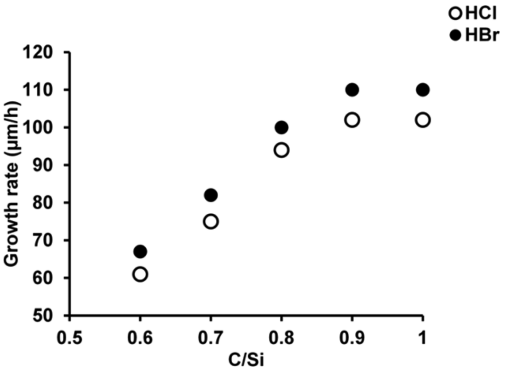

Figure 4. Dependence of growth rate on the C/Si ratio with Si/H_2 = 0.25% and (Cl or Br)/Si = 4 for chlorinated and brominated chemistry for 4H-SiC epitaxial growth.

The C/Si has also proven to be of high importance for controlling the surface roughness in homoepitaxial SiC growth.[30] The surface roughness, quantified by the root-mean-square (RMS) values of 20 × 20 μm^2 AFM scans, for C/Si ratios between 0.6 and 1 is plotted in Figure 5. Low surface roughness is obtained for both chlorinated and brominated chemistry at C/Si ≥ 0.8. At C/Si ratio of 0.7, the surface morphology deteriorates, as seen by the RMS values of 3.22 and 3.33 nm for chlorinated and brominated growth, respectively. This very rough surface is a well-documented

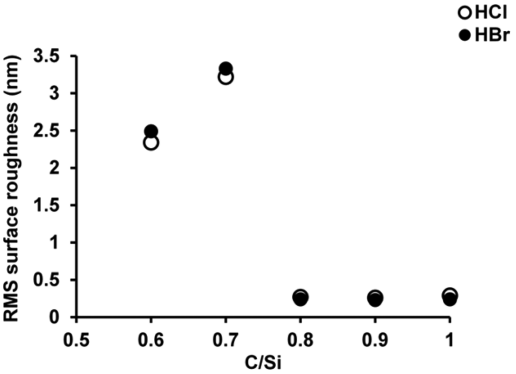

Figure 5. Dependence of RMS value on the C/Si ratio with Si/H_2 = 0.25% and (Cl or Br)/Si= 4 for chlorinated and brominated chemistry for 4H-SiC epitaxial growth. The thickness of the layers range from 15 μm at C/Si = 0.6 to 27 μm at C/Si = 1.

DOI: 10.1021/acs.chemmater.5b00074
Chem. Mater. 2015, 27, 793−801

phenomenon known as step bunching caused by higher growth rate at atomic terraces than at atomic steps.[31] At silicon rich conditions, step bunching is believed to be caused by formation of Si clusters on the step terraces on the surface.[32] The somewhat reduced surface roughness at C/Si = 0.6 compared to C/Si = 0.7 is due to a reduction in growth rate, from 75 to 61 μm/h for chlorinated growth and from 82 to 67 μm/h for brominated growth. This reduction in growth rate is in line with previous reports[33] and is caused by the lower carbon supply to the surface.

AFM images of 25 and 27 μm thick epitaxial layers grown by chlorinated and brominated chemistry, respectively, at C/Si = 0.9 are given in Figure 6a. The RMS surface roughness values are 0.26 nm for chlorinated chemistry and 0.23 nm for brominated chemistry. For comparison, the 4H-SiC unit cell height in the c direction is 1.016 nm. For comparison are AFM images of epitaxial layers grown at C/Si = 0.7, resulting in surfaces with step bunching shown in Figure 6b. Optical microscopy images showing an overview of the epitaxial layer surfaces are shown in Figure 6c, the density of the triangular defects commonly seen for homoepitaxial growth of SiC on 4° off axis substrates was 1−3 cm^{-2}, regardless of chlorinated or brominated chemistry.

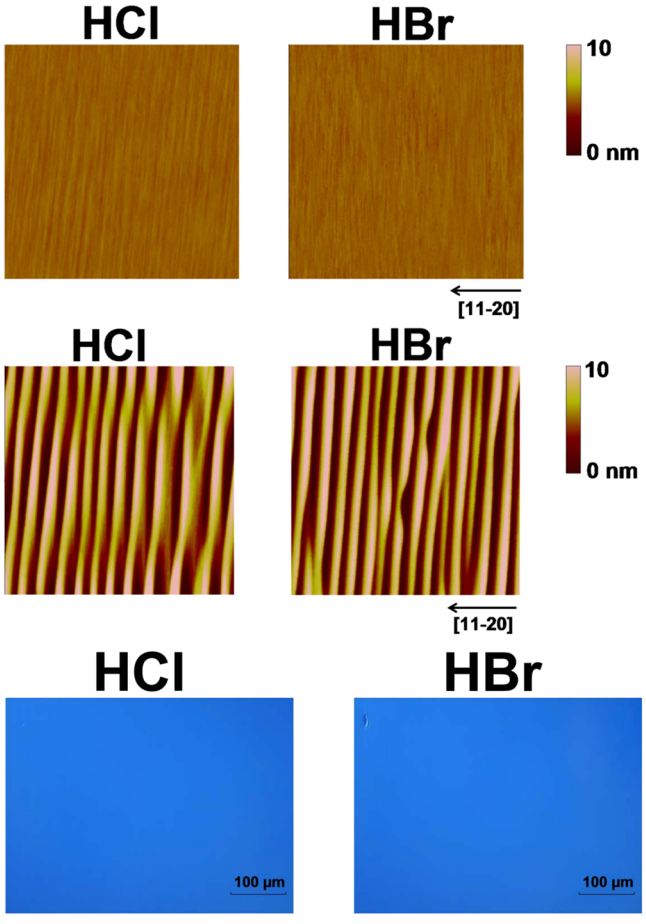

Figure 6. Surface morphology of epitaxial SiC layers grown with chlorinated and brominated chemistry. (a) AFM images (20 × 20 μm^2) for homoepitaxial layers grown by chlorinated and brominated chemistry at C/Si = 0.9 and Si/H_2 = 0.25%, having RMS values of 0.26 and 0.23 nm, respectively. (b) AFM images (20 × 20 μm^2) for homoepitaxial layers grown by chlorinated and brominated chemistry Si/H_2 = 0.25% and C/Si = 0.7, resulting in a step-bunched surface having RMS values of 3.33 and 3.22 nm, respectively. (c) Optical microscopy images of the SiC epitaxial layer surface grown with HCl and HBr addition with C/Si = 0.9. The thicknesses of the epitaxial layers are around 25 μm.

The results from the above experiments, with a fixed (Cl or Br)/Si ratio, all suggests very similar CVD processes for both HBr and HCl addition and that either halogen could be used as additive in SiC CVD. In an effort to unravel differences in the halogenated chemistries, the effect of (Cl or Br)/Si on the growth rate was investigated by experiments where the (Cl or Br)/Si was varied between 4 and 8, keeping Si/H_2 = 0.25% and C/Si = 1 (Figure 7). Here a difference between the two

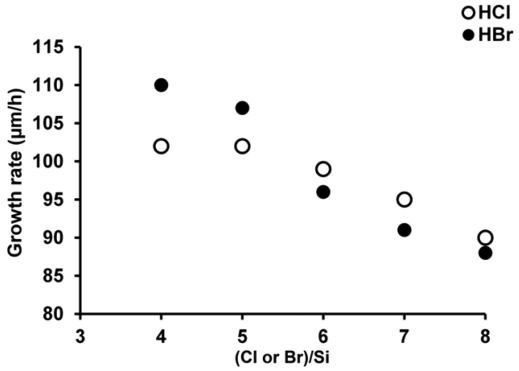

Figure 7. Dependence of growth rate on the Cl/Si and Br/Si ratio with Si/H_2 = 0.25% and C/Si = 1 for chlorinated and brominated chemistries.

halogens can be noted. As expected, the growth rate decreases with both higher Cl/Si and higher Br/Si. This has been observed earlier for chlorinated chemistry and is ascribed to increased etching by the higher HCl concentration during growth.[34] The growth rate shows a very similar dependence for the Cl/Si and the Br/Si ratios at (Cl or Br)/Si ≥ 6. The growth rate is here somewhat lower for brominated chemistry, indicating a higher etching rate. At (Cl or Br)/Si ≤ 5, the growth rate is instead higher for brominated chemistry, suggesting that in this region with lower etching, the brominated chemistry gives a higher supply of silicon to the SiC surface. Such a change in the effective C/Si ratio above the SiC surface could be reflected in the doping of the grown material as nitrogen incorporation drops with higher C/Si.[28] But because nitrogen incorporation also has been shown to increase with Cl/Si,[35] the net carrier concentration of the layers is not a good indicator of the effective C/Si ratio at different (Cl or Br)/Si ratios.

The surface roughness of the grown epitaxial layers increased somewhat for higher (Cl or Br)/Si; RMS values of 0.24, 0.29, and 0.31 for Br/Si of 4, 6, and 8 respectively and 0.29, 0.33, and 0.36 for Cl/Si of 4, 6, and 8 respectively were recorded. Etching experiments, without silicon or carbon precursors added, confirmed a higher etching rate for HBr compared to HCl, the experiments showed etching rates of 85 nm/min for HCl and 100 nm/min for HBr. The higher etching rate for HBr compared to HCl could be due to the lower energy barrier for desorption of $SiBr_2$ compared to $SiCl_2$, as found by our quantum chemical calculations described below.

Secondary ion mass spectrometry (SIMS) was employed in attempt to compare bromine and chlorine incorporation in the grown epitaxial layers. However, it was found that both the bromine and chlorine content in the epitaxial layers were below

DOI: 10.1021/acs.chemmater.5b00074
Chem. Mater. 2015, 27, 793−801

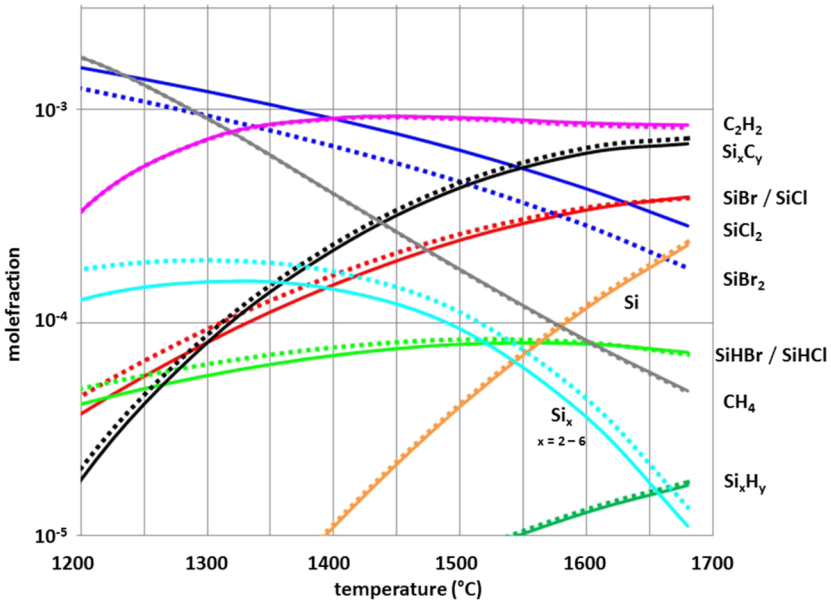

Figure 8. Mole fractions of the most abundant species at thermodynamic equilibrium vs temperature. Solid lines represent the Si−C−Cl−H system, whereas dotted lines represent the Si−C−Br−H system.

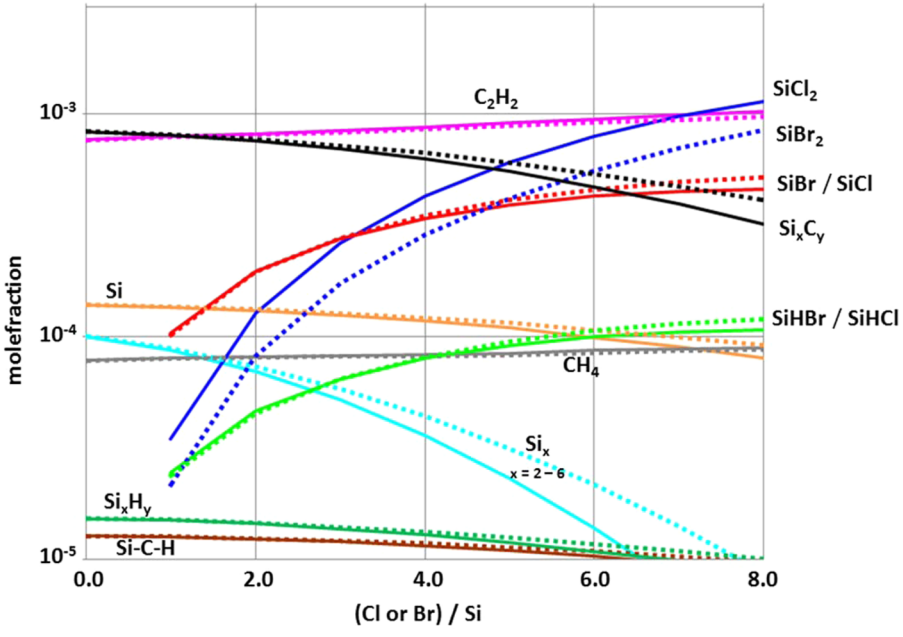

Figure 9. Mole fractions of the most abundant species at thermodynamic equilibrium (at 1600 °C) vs Cl/Si ratio or Br/Si ratio, respectively. Solid lines represent the Si−C−Cl−H system, whereas dotted lines represent the Si−C−Br−H system.

the SIMS detection limit of 2×10^{14} cm^{-3} pointing to a very low incorporation. It has been suggested that minute incorporation of halogen atoms can alter the electronic properties of SiC; Cl in the SiC lattice was claimed to create three new traps in n-type 4H-SiC epitaxial layers at E_C −0.37 eV, E_C −1.06 eV, and E_C −1.3 eV and one new level in p-type at E_V +0.97.[36]

Gas Phase Chemistry for Growth with Chlorinated and Brominated Chemistry. Calculations of thermodynamic equilibrium were made for a gas mixture composition of Si/H_2 = 0.25%, C/Si = 1.0, and Cl/Si = 4.0 or Br/Si = 4.0, and a pressure of 100 mbar. Species equilibrium mole fractions vs temperature (Figure 8) show that, at growth temperatures (1500−1600 °C), most of the silicon is in the form of small Si_xC_y species, with Si_2C being the dominating one, and Si_3C contributing with about 5% to the total Si_xC_y concentration. Most of the carbon is in the form of C_2H_2, in agreement with previous literature,[37] but also with a large contribution from the Si_xC_y species (mainly Si_2C and Si_3C). Among the halogenated species, SiX, SiX_2 and SiHX (X = Cl or Br) are the ones highest in concentration at normal SiC CVD conditions. It is also noted that although some silicon clusters (Si_x, with $x > 2$) are formed at lower temperatures, they rapidly decompose above 1400 °C.

Increasing the halogen atom concentration (Cl or Br) results in a large increase for SiX_2 over the interval studied here (Figure 9). It is also noted that in the Si−C−Cl−H system, the species not containing chlorine decrease more with increasing

DOI: 10.1021/acs.chemmater.5b00074
Chem. Mater. 2015, 27, 793−801

Table 1. Reaction Energies for Reactions between $SiH_2/SiBr_2/SiCl_2$ and the Hydrogen-Terminated (000-1) 4H-SiC Surface[a]

reaction	reaction energy ΔE (kJ mol^{-1})		
	X = H	X = Br	X = Cl
$SiX_2(g) + H(ads) \rightarrow SiX_2(ads) + \frac{1}{2}H_2(g)$ (1)	−57	9	27
$SiX_2(g) + 2H(ads) \rightarrow SiX_2(ads) + H_2(g)$ (2)	−14	69	105
$2SiX_2(g) + 2H(ads) \rightarrow 2SiX_2(ads) + H_2(g)$ (3)	−395	−256	−184
$SiX_2(g) + H(ads) \rightarrow SiX_2H(ads)$ (4)	−214	−128	−123

[a]Note that there is some interaction between the two adsorbed $SiBr_2$ in (3), making the reaction more exothermic per $SiBr_2$ than (1).

Cl concentration as compared to the same species in the Br case. This can be attributed to the stronger Si−Cl bond, which will "attract" more of the silicon otherwise bonded in other molecules. As a result, all Si containing species without Cl or Br, have higher mole fractions in the Br case, and the difference is larger at higher halogen concentration.

It has been argued that the main silicon species for SiC growth with chlorinated CVD chemistry is $SiCl_2$,[38] which is due to the molecular similarity to SiH_2, which is argued to be the main silicon species in the standard, nonhalogenated SiC CVD chemistry.[39] Given this suggested chemical model, the approximately 10% higher growth rate observed for the brominated chemistry (Figure 2) is not immediately evident from the thermochemical calculations. Of the halogenated species in Figure 8, the Br-containing species have similar concentrations as the corresponding Cl-species with the exception of $SiBr_2$, which has a lower concentration than $SiCl_2$. Moreover, the Br-containing species are heavier, which lead to slower movements and thus lower impingement rates on the surface. This would imply lower growth rates in the brominated chemistry, as compared to the chlorinated chemistry. Therefore, to explain the higher growth rates for brominated chemistry one could suggest that (i) the gas-phase reactions leading to formation of SiX_2 and SiX are faster when X = Br compared to when X = Cl or (ii) there is a substantially higher contribution to growth from nonhalogen molecules, and much less contribution from the halogenated molecules, than previously pictured.

The arguments for (i) is that the equilibrium calculations (Figure 9) show higher mole fractions of silicon chlorides as compared to silicon bromides. When calculating the impact rate of molecules at the growth surface, the difference is even larger due to the difference in weight (Br is heavier than Cl, thus the impact rate will be lower according to eq 1. Therefore, if we assume these molecules to be the main contributors, the gas-phase reactions leading to their formation should be faster in the bromide case. If considering (ii), the equilibrium calculations show that brominated chemistry yields higher mole fractions for molecules without halogen atoms, as compared to the same molecules in the chloride case. Taking the ratio of the molecular impact rate with the surface for these molecules in the two cases gives approximately 1.1 at 1600 °C, in favor for Br. Thus, the growth rate would be 10% higher for Br, as seen from experiments (Figure 2). This, however, requires that the halogenated molecules play a much smaller role in the growth of SiC and thus that the view on halogenated SiC CVD chemistry needs to be changed. A possible alternative chemical mechanism would thus be that Si_2C (and possibly also Si_3C) together with C_2H_2 are the species responsible for SiC growth and that the addition of halogens only serve to suppress the formation of Si clusters in the gas phase by formation of SiX_2, SiX, and SiHX where X is a halogen, but that these halogenated species are not contributing to the SiC growth.

Surface Chemistry with Chlorinated and Brominated Chemistry. To explain the higher etching observed for brominated chemistry compared to chlorinated chemistry, we used quantum chemical computations of the adsorption reactions for SiH_2, $SiCl_2$, and $SiBr_2$ on the 4H-SiC (000−1) surface. These calculations have previously been done for $SiCl_2$ and SiH_2 to probe the effect of chlorinated chemistry on the growth surface chemistry.[17] Although the above thermochemical calculations suggests that the SiX_2 species (X = Cl or Br) are not active in SiC growth, they are likely active in SiC etching given their sharp increase with higher (Cl or Br)/Si (Figure 9). Calculated reaction energies for adsorption reactions between the hydrogen terminated 4H-SiC (000−1) surface and $SiH_2/SiCl_2/SiBr_2$ are summarized in Table 1 and Figure 10. Etching of the SiC surface in standard/chlorinated/brominated chemistries can be regarded as the reverse of these adsorption reactions. The adsorption energies obtained are ordered as $\Delta E(SiH_2) < \Delta E(SiBr_2) < \Delta E(SiCl_2)$. The $SiCl_2$ and $SiBr_2$ molecules show a very similar behavior for all reactions 1−4 in Table 1, especially for reaction 4 where the energies for $SiBr_2$ and $SiCl_2$ are very similar. Reaction 4 is the reaction which gives the strongest adsorption per SiX_2 (X = H, Cl, or Br) and could thus be regarded as most probable and therefore studied in more detail in Figure 10.

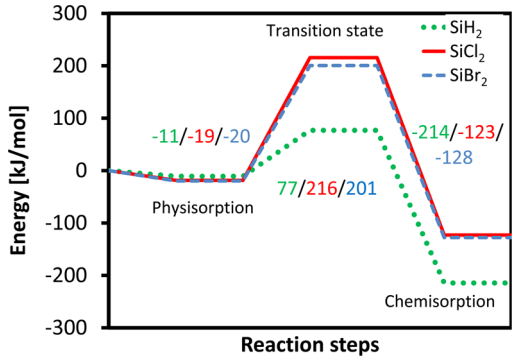

Figure 10. Reaction paths for reaction 4. In Table 1. Reaction energies for SiX_2 where X = H, Cl, Br are given for $SiH_2/SiCl_2/SiBr_2$, correspond to the energies for reaction 4 in Table 1

From Figure 10, one can see that the activation energy for adsorption of $SiBr_2$ is slightly lower than for the $SiCl_2$ molecule but much higher than for the SiH_2 molecule. The somewhat lower transition state energy for the reaction with $SiBr_2$ compared to $SiCl_2$ implies that when etching occurs by formation of a chemisorbed SiX_2 (X = H, Cl, or Br) from a

DOI: 10.1021/acs.chemmater.5b00074
Chem. Mater. 2015, 27, 793−801

chemisorbed Si atom, a brominated chemistry should allow for easier desorption of the SiX_2 compared to a chlorinated chemistry, which can explain the somewhat higher etching rate observed for brominated chemistry.

Precursor Considerations. This study has compared chlorinated and brominated CVD chemistries for SiC by using HCl respectively HBr as additive. As previously outlined,[8] chlorinated chemistry offers a wide range of commercially available precursor routes for Cl addition besides HCl addition; the standard precursors, SiH_4 and C_2H_4, can be replaced by a chlorinated alternatives, SiH_xCl_y, CH_xCl_y, or a single molecule approach can be used, $SiH_xC_yCl_z$. Especially, the availabilities of high-purity chlorinated silanes, mainly $SiCl_4$ and $SiHCl_3$, is largely due to their widespread use in the silicon industry. Brominated chemistry does not offer this wide range of options and is therefore perhaps less attractive at a first glance. However, in a recent study, we have shown that for a combination of both high growth rate and high-quality morphology, HCl addition to the standard precursors is the best chemical route for chlorinated chemistry.[40] In the light of this study, brominated chemistry by HBr addition can be viewed as a solid alternative to HCl addition. An advantage of brominated chemistry is that the Br_2 byproduct, mainly formed as the gas mixture cools downstream from the growth chamber, should be relatively easy to remove by a cold trap. Removal of Cl_2 requires scrubbing of the gas mixture by alkaline water solution or solid state scrubbing by, for example, KOH (s).

■ CONCLUSIONS

Our results show that brominated and chlorinated chemistries gives very similar results in terms of material quality, growth rate, doping and morphology of the homoepitaxially grown SiC layers and that the CVD gas phase chemistries are very similar. A somewhat higher growth rate was noted for brominated chemistry, which thus points to that brominated chemistry could be a better choice than chlorinated chemistry. Our thermochemical modeling of the gas-phase chemistry further suggests that the chemical mechanism for chlorinated SiC CVD used today based on $SiCl_2$ as the major Si-containing species for SiC growth is possibly wrong and that Si_2C is the major Si species contributing to SiC growth.

■ ASSOCIATED CONTENT

Supporting Information

A list over the species included in the thermochemical calculations and thermochemical data from quantum chemical calculations. This material is available free of charge via the Internet at http://pubs.acs.org.

■ AUTHOR INFORMATION

Corresponding Author

*E-mail: henrik.pedersen@liu.se. Twitter: @hacp81.

Notes

The authors declare no competing financial interest.

■ ACKNOWLEDGMENTS

The authors gratefully acknowledge the financial support from Swedish Energy Agency, Swedish Foundation for Strategic research (SSF), and the Swedish Research Council (VR).

■ REFERENCES

(1) Matsunami, H.; Kimoto, T. *Mater. Sci. Eng. R* **1997**, *20*, 125.
(2) Elasser, A.; Chow, T. P. *Proc. IEEE* **2002**, *90*, 969.
(3) Kordina, O.; Hallin, C.; Henry, A.; Bergman, J. P.; Ivanov, I.; Ellison, A.; Son, N. T.; Janzén, E. *Phys. Status Solidi B* **1997**, *202*, 321.
(4) Cooper, J. A.; Agarwal, A. *Proc. IEEE* **2002**, *90*, 956.
(5) La Via, F.; Galvagno, G.; Foti, G.; Mauceri, M.; Leone, S.; Pistone, G.; Abbondanza, G.; Veneroni, A.; Masi, M.; Valente, G. L.; Crippa, D. *Chem. Vap. Deposition* **2006**, *12*, 509.
(6) Ellison, A.; Zhang, J.; Henry, A.; Janzén, E. *J. Cryst. Growth* **2002**, *236*, 225.
(7) Ito, M.; Storasta, L.; Tsuchida, H. *Appl. Phys. Express* **2008**, *1*, 015001.
(8) Pedersen, H.; Leone, S.; Kordina, O.; Henry, A.; Nishizawa, S.; Koshka, Y.; Janzén, E. *Chem. Rev.* **2012**, *112*, 2434.
(9) All bond enthalpies from: *CRC Handbook of Chemistry and Physics*, 95th ed.; CRC Press: Boca Raton, FL, 2014.
(10) Rana, T.; Chandrashekar, M. V. S.; Sudarshan, T. S. *Phys. Status Solidi A* **2012**, *209*, 2455.
(11) Kunstmann, Th.; Anger, H.; Knecht, J.; Veprek, S.; Mitzel, N. W.; Schmidbaur, H. *Chem. Mater.* **1995**, *7*, 1675.
(12) Kunstmann, Th.; Veprek, S. *Appl. Phys. Lett.* **1995**, *67*, 3126.
(13) Henry, A.; Hassan, J.; Bergman, J. P.; Hallin, C.; Janzén, E. *Chem. Vapor Deposition* **2006**, *12*, 475.
(14) (a) Allendorf, M. D. *J. Electrochem. Soc.* **1993**, *140*, 747. (b) Deng, J. L.; Su, K. H.; Wang, X.; Zeng, Q. F.; Cheng, L. F.; Xu, Y. D.; Zhang, L. T. *Eur. Phys. J. D* **2008**, *49*, 21. (c) Deng, J.; Su, K.; Zeng, Y.; Wang, X.; Zeng, Q.; Cheng, L.; Xu, Y.; Zhang, L. *Physica A* **2008**, *387*, 5440.
(15) Allendorf, M. D.; Melius, C. F. *J. Phys. Chem.* **1993**, *97*, 720.
(16) Cooke, M. J.; Harris, G. *J. Vac. Sci. Technol. A* **1989**, *7*, 3217.
(17) Kalered, E.; Pedersen, H.; Janzén, E.; Ojamäe, L. *Theor. Chem. Acc.* **2013**, *132*, 1403.
(18) (a) Becke, A. D. *J. Chem. Phys.* **1993**, *98*, 5648. (b) Lee, C.; Yang, W.; Parr, R. G. *Phys. Rev. B* **1988**, *37*, 785.
(19) Hehre, W. J.; Ditchfield, R.; Pople, J. A. *J. Chem. Phys.* **1972**, *56*, 2257.
(20) Frisch, M. J.; Trucks, G. W.; Schlegel, H. B.; Scuseria, G. E.; Robb, M. A.; Cheeseman, J. R.; Scalmani, G.; Barone, V.; Mennucci, B.; Petersson, G. A.; Nakatsuji, H.; Caricato, M.; Li, X.; Hratchian, H. P.; Izmaylov, A. F.; Bloino, J.; Zheng, G.; Sonnenberg, J. L.; Hada, M.; Ehara, M.; Toyota, K.; Fukuda, R.; Hasegawa, J.; Ishida, M.; Nakajima, T.; Honda, Y.; Kitao, O.; Nakai, H.; Vreven, T.; Montgomery Jr, J. A.; Peralta, J. E.; Ogliaro, F.; Bearpark, M.; Heyd, J. J.; Brothers, E.; Kudin, K. N.; Staroverov, V. N.; Kobayashi, R.; Normand, J.; Raghavachari, K.; Rendell, A.; Burant, J. C.; Iyengar, S. S.; Tomasi, J.; Cossi, M.; Rega, N.; Millam, J. M.; Klene, M.; Knox, J. E.; Cross, J. B.; Bakken, V.; Adamo, C.; Jaramillo, J.; Gomperts, R.; Stratmann, R. E.; Yazyev, O.; Austin, A. J.; Cammi, R.; Pomelli, C.; Ochterski, J. W.; Martin, R. L.; Morokuma, K.; Zakrzewski, V. G.; Voth, G. A.; Salvador, P.; Dannenberg, J. J.; Dapprich, S.; Daniels, A. D.; Farkas, O.; Foresman, J. B.; Ortiz, J. V.; Cioslowski, J.; Fox, D. J. *Gaussian 09*; Gaussian, Inc.: Wallingford, CT, 2009.
(21) Standard thermodynamic data from: *CRC Handbook of Chemistry and Physics*, 95th ed.; CRC Press: Boca Raton, FL, 2014.
(22) (a) Peng, C.; Ayala, P. Y.; Schlegel, H. B.; Frisch, M. J. *J. Comput. Chem.* **1996**, *17*, 49. (b) Peng, C.; Schlegel, H. B. *Israel J. Chem.* **1993**, *33*, 449.
(23) Halgren, T. A.; Lipscomb, W. N. *Chem. Phys. Lett.* **1977**, *49*, 225.
(24) Ivanov, I. G.; Hallin, C.; Henry, A.; Kordina, O.; Janzén, E. *J. Appl. Phys.* **1996**, *80*, 3504.
(25) Pedersen, H.; Leone, S.; Henry, A.; Darakchieva, V.; Carlsson, P.; Gällström, A.; Janzén, E. *Phys. Status Solidi RRL* **2008**, *2*, 188.
(26) Larkin, D. J. *Phys. Status Solidi B* **1997**, *202*, 305.
(27) Larkin, D. J.; Neudeck, P. G.; Powell, J. A.; Matus, L. G. *Appl. Phys. Lett.* **1994**, *65*, 1659.
(28) Forsberg, U.; Danielsson, Ö.; Henry, A.; Linnarsson, M. K.; Janzén, E. *J. Cryst. Growth* **2002**, *236*, 101.
(29) Kimoto, T.; Nishino, H.; Yoo, W. S.; Matsunami, H. *J. Appl. Phys.* **1993**, 73.

DOI: 10.1021/acs.chemmater.5b00074
Chem. Mater. 2015, 27, 793−801

(30) Yazdanfar, M.; Pedersen, H.; Sukkaew, P.; Ivanov, I. G.; Danielsson, Ö.; Kordina, O.; Janzén, E. *J. Cryst. Growth* **2014**, *390*, 24.
(31) Kimoto, T.; Itoh, A.; Matsunami, H.; Okano, T. *J. Appl. Phys.* **1997**, *81*, 3494.
(32) Ishida, Y.; Takahashi, T.; Okumura, H.; Arai, K.; Yoshida, S. *Mater. Sci. Forum* **2009**, *600*−*603*, 473.
(33) Yazdanfar, M.; Ivanov, I. G.; Pedersen, H.; Kordina, O.; Janzén, E. *J. Appl. Phys.* **2013**, *113*, 223502.
(34) Pedersen, H.; Leone, S.; Henry, A.; Lundskog, A.; Janzén, E. *Phys. Status. Solidi. RRL* **2008**, *2*, 278.
(35) Pedersen, H.; Beyer, F. C.; Hassan, J.; Henry, A.; Janzén, E. *J. Cryst. Growth* **2009**, *311*, 1321.
(36) Alfieri, G.; Kimoto, T. *J. Appl. Phys.* **2012**, *112*, 063717.
(37) This is reported for most papers on SiC CVD modelling but the most original reference is Stinespring, C. D.; Wormhoudt, J. C. *J. Cryst. Growth* **1988**, *87*, 481.
(38) Pedersen, H. Talk given during the European Conference on Silicon Carbide and Related Materials (ECSCRM), 7−11 September 2008, Barcelona, Spain. Conference proceedings paper: Pedersen, H.; Leone, S.; Henry, A.; Beyer, F. C.; Lundskog, A.; Janzén, E. *Mater. Sci. Forum* **2009**, *615*−*617*, 89.
(39) Allendorf, M. D.; Kee, J. *J. Electrochem. Soc.* **1991**, *138*, 841.
(40) Yazdanfar, M.; Danielsson, Ö.; Kordina, O.; Janzén, E.; Pedersen, H. *ECS J. Solid State Sci. Technol.* **2014**, *3*, P320.

DOI: 10.1021/acs.chemmater.5b00074
Chem. Mater. 2015, 27, 793−801